Structural and electrical investigation of Al/Ti/TiN/Au based N-face n-GaN contact stack

Zsolt Fogarassy [a,**], Aleksandra Wójcicka [b], Ildikó Cora [a], Adel Sarolta Rácz [a,*],
Szymon Grzanka [c], Erzsébet Dodony [a], Piotr Perlin [d], Michał A. Borysiewicz [b,***]

[a] HUN-REN Centre for Energy Research, Institute for Technical Physics and Materials Science, Budapest, Hungary
[b] Łukasiewicz Research Network – Institute of Microelectronics and Photonics, Warsaw, Poland
[c] TOP-GAN, Warsaw, Poland
[d] Institute of High Pressure Physics, Polish Academy of Sciences, Warsaw, Poland

ARTICLE INFO

ABSTRACT

In this work, the structure of Ti/Al/TiN/Au contact layer stack on the N-face of a single-crystal n-GaN substrate is studied after heat treatment at 750 °C. Since TiN is widely regarded as a diffusion barrier in the stack, the formed structures with three different initial TiN thicknesses (15, 60 and 90 nm) in the contact layers are investigated in detail. The primary tool used for the structural investigations was a (scanning) transmission electron microscope ((S)TEM). In all three samples a low resistivity ohmic contact was formed. However, the TiN layer has not completely blocked the diffusion for any of the samples and both Al and Au diffused through the TiN layer at the temperature of 750 °C. As a result of the heat treatment, a complex $AlN/TiN/Au_2Al/TiN/Au + Al_{2.67}O_4$ stack was formed on the surface of the GaN substrate. The measurements have not shown the often reported Ti–Al alloy phase in the samples. The formation of the AlN and TiN layers can be explained by the separation of N from GaN creating N vacancies in the GaN substrate which could help the formation of the ohmic behavior.

1. Introduction

Gallium nitride (GaN) is a direct bandgap semiconductor which has been applied in blue laser diodes (LD) since the 1990s. Due to its special properties, GaN can be used for special optical devices, high-power and high-frequency devices such as purple lasers, high-voltage switching devices and GaN-based high electron mobility transistors (HEMT) [1]. While the high frequency devices utilize heteroepitaxial n-type GaN based structures with all the exposed surfaces being of Ga-face polarity, high power and optical devices perform better if they are executed as vertical devices with p-type GaN structures grown homoepitaxially on bulk n-GaN substrates, in which case the bottom side is usually the N-polar n-type GaN, whereas the top side is usually the Ga-face p-type GaN. The production of bulk GaN single crystals has been successfully achieved making it possible to obtain bulk GaN single crystals commercially fueling the development of high power and optoelectronic devices. An important task in the production of GaN-based vertical devices is to establish the appropriate electrically conductive contact to a specific conductivity type on the Ga or N polar sides of the GaN single crystal. Due to the different chemical properties of both polarities, the metallurgical reactions between the contact metallizations and the gallium nitride face might take place differently. In particular, the contact formation to Ga-face n-GaN (*e.g.* in HEMT) and N-face n-GaN (*e. g.* in LD) might not always yield the same results even for the same applied metallizations [2].

The very first ohmic contact stack which has become widespread for GaN-based devices is the Ti/Al bilayer [3]. According to the most widespread view, the Ti layer deposited on the GaN yields the out-diffusion of some nitrogen from the GaN after thermal treatment, thereby creating nitrogen vacancies [1]. These vacancies created in GaN can act as shallow donors yielding a highly conducting n + subcontact layer improving the contact resistivity [4]. There are others who believe that the phase of the resulting Ti–Al alloy causes the good ohmic behavior [5]. Another advantage of the Al layer is that it absorbs oxygen
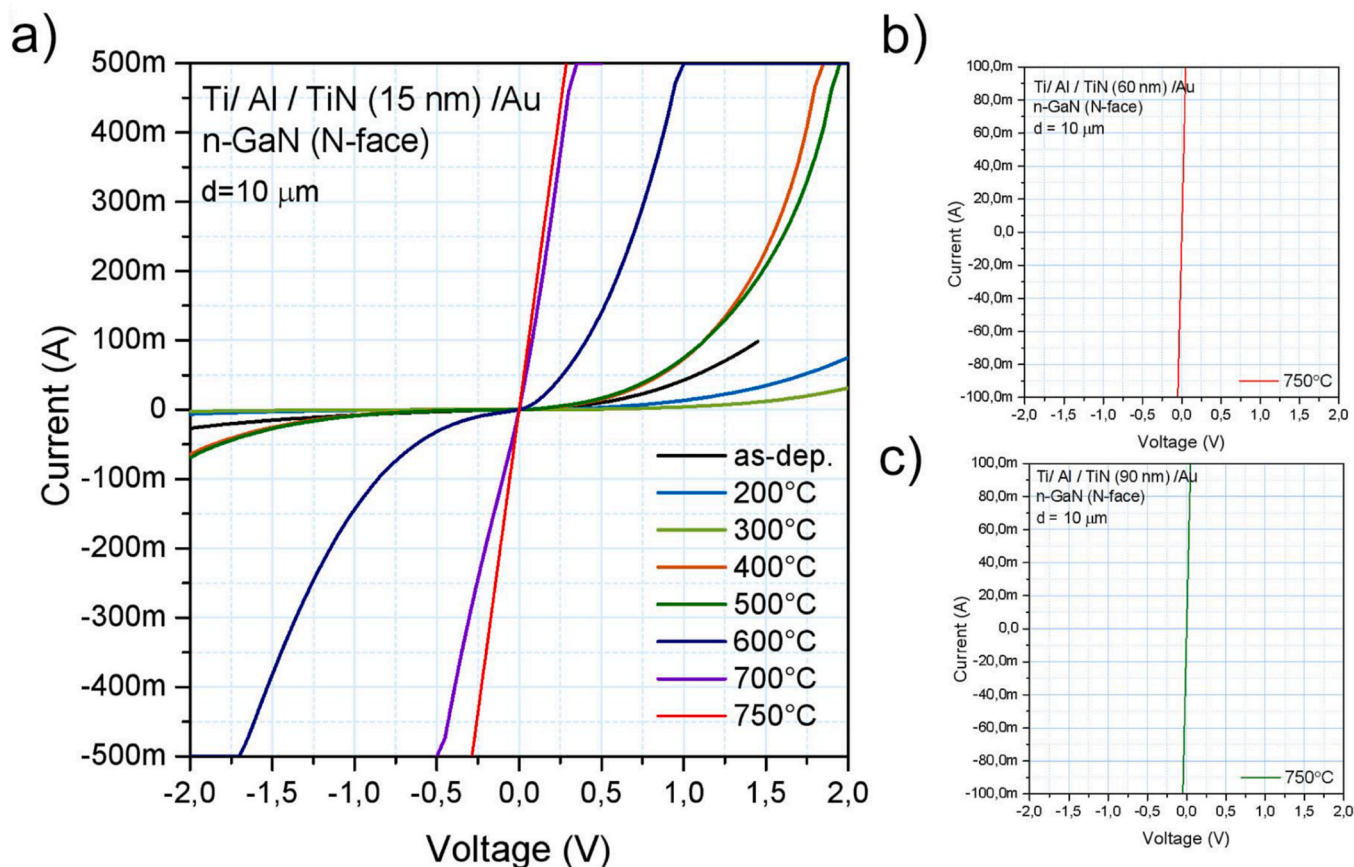

Fig. 1. I–V characteristics measured using circular TLM structures in Ti/Al/TiN/Au contact with (a) 15 nm – thick TiN layer at different annealing temperatures, (b) 60 nm-thick TiN annealed at 750 °C and (c) 90 nm-thick TiN after heat treatment at 750 °C.

contamination from the Ti layer during heat treatment [6]. The Al/Ti layer is most often provided with an Au layer for external wire contact. However, according to the investigations, the Au layer can spoil the surface morphology making the surface rough during the heat treatment [7] and Al–Au alloy can be also formed [8]. Diffusion-inhibiting interlayers between the Al and Au layer are applied to prevent the oxidation of the contact layer and the diffusion of Al and Au. One of the more frequently used interlayers is TiN [9,10]. Since the Al/Ti/TiN/Au stack is heated up above 700 °C for forming the ohmic contact many studies focused on the structural investigations but usually without Au contacting layer on the top [8,11], or if there was Au on the surface, no TiN was used [12] or Mo was used instead of TiN [13]. There are works where Al was not used, only Ti was deposited on the GaN [14]. Observations also vary, sometimes AlN is seen on the surface of GaN and according to the authors, Ti can play a catalytic role to form AlN [15]. In some studies, Al is left out and Ti is deposited in two steps, and with that method they could still achieve good ohmic conductivity [16]. Due to the limited studies, we decided to investigate full Ti/Al/TiN/Au contact stacks before and after contact formation and to study the role of the TiN layer as a diffusion-blocking layer in depth during contact formation.

The TiN can be effective as a diffusion barrier layer depending on the temperature, diffusing material [17,18] and on the structure of TiN [19]. TiN is not a high-temperature diffusion blocking layer, it typically works effectively up to 500–700 °C depending on the applied materials [17–19]. However the Ti/Al/TiN/Au layers on the GaN substrate are typically heat-treated at temperatures above 700 °C to achieve proper conductivity [1]. In some applications the GaN-based device may approach this temperature during use, therefore it is of particular interest to understand exactly what kind of layers form on GaN after the heat treatment.

Herein, we present the investigations of the Ti/Al/TiN/Au ohmic contact formed by heat treatment at 750 °C on the N-face of a single-crystal n-GaN substrate. The role and the thickness of the TiN layer is especially underlined in this study. The measurements were primarily carried out using the cross-sectional (scanning) transmission electron microscope ((S)TEM) method.

2. Experimental section

GaN substrates grown by single crystal halide vapor phase epitaxy (HVPE) were used for the metallization deposition. The material exhibited electron concentration of $1 \cdot 10^{18}$ cm^{-3}, resistivity of 20 mΩcm and average thickness of 330 μm. An extensive preparation of the substrates had to be applied before the metallization stack deposition for obtaining optimal results. As a first step, mechano-chemical polishing with colloidal silica suspension was conducted to achieve the atomically flat n-GaN N-face. Subsequently, the substrates were cleaned in the following sequence of organic solutions: (1) trichloroethylene at 75 °C, (2) acetone with ultrasound added, (3) isopropanol at 75 °C and (4) isopropanol at room temperature. Finally, they were rinsed with deionized H$_2$O and blown dry with nitrogen. Each immersion lasted 5 min. Then, 400 nm of the N-face side was removed using a BCl$_3$/Cl$_2$ inductively coupled plasma (ICP) in an Oxford Instruments Plasmalab System 100 reactor. The samples prepared for contact characterization were patterned using UV lift-off lithography in circular transmission line method (cTLM) patterns. Native oxide was removed from each sample directly before metal deposition, also from the patterned samples, by a 1 min bath in a 1:2 HCl:H$_2$O solution at room temperature, followed by a 3 min deionized water rinse and nitrogen blow dry. Ohmic contact metallizations have been deposited by e-beam evaporation using a
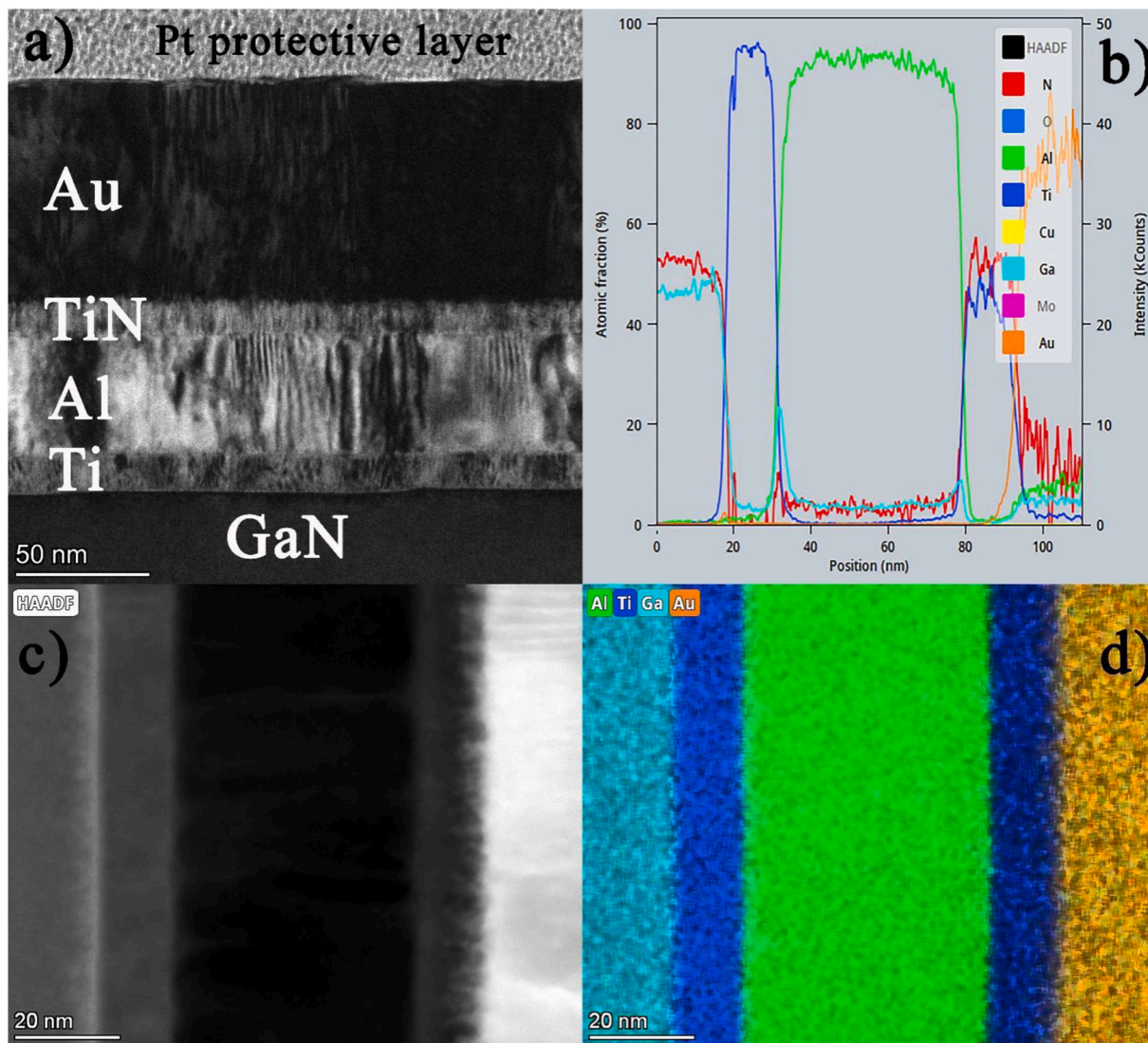
Fig. 2. The bright-field (BF) TEM image (a), HAADF (high angle annular dark field) image (c), Al, Ti, Ga, Au element map (d) and the integral element distribution parallel to the surface (b) obtained from the non-heat-treated sample containing 15 nm thick TiN layer. The Ga in the contact layer is a thinning artifact shown in image b).
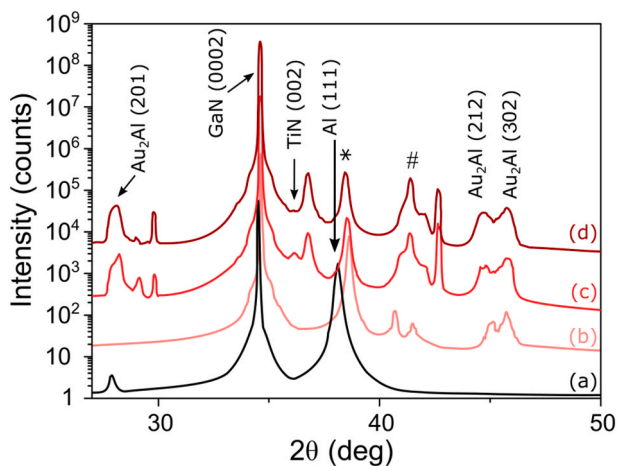

Fig. 3. XRD diffraction patterns of the as-deposited sample (a) and heat-treated 15 nm TiN (b), 60 nm TiN (c) and 90 nm TiN (d) samples. * denotes Au (111), Au_2Al (210), # denotes Au_2Al (203), Au_2Al (004) (Au_2Al with Pnna (62) sg.).

TFDS-462U system from V.S.T. Ltd. We deposited the following sequence of the contact stack layers: Ti/Al/TiN/Au, with thickness of $15/60/x/50$ nm, respectively. Three samples with different thickness (x) of TiN layer were prepared: 15 nm, 60 nm and 90 nm. The analyses of contact structures were conducted based on four samples, one with the standard 15 nm-thick TiN without additional heat treatment (as-deposited) and three others, containing: 15 nm-thick, 60 nm-thick and 90 nm-thick TiN, all three annealed at 750 °C in nitrogen for 90 s. The contact formation temperature was established after the sample with the thinnest TiN layer was annealed in the range of 200–750 °C with a step of 100 °C in a nitrogen atmosphere for 90 s per step. The annealing was performed in a Mattson SHS 100 rapid thermal processing furnace.

The current-voltage (I–V) characteristics of the contacts were measured using a Keithley 2400 source-meter using a simple probe-station. The cTLM pads could be used to determine the contact evolution, however the cTLM approach was insufficient for accurately determining the very low contact resistivities of the samples exhibited after formation at 750 °C.

The crystalline structure and phase evolution after annealing of the contact stacks was determined using X-ray diffraction with a Cu-lamp and a Bragg-Brentano configuration on a PANalytical Empyrean.
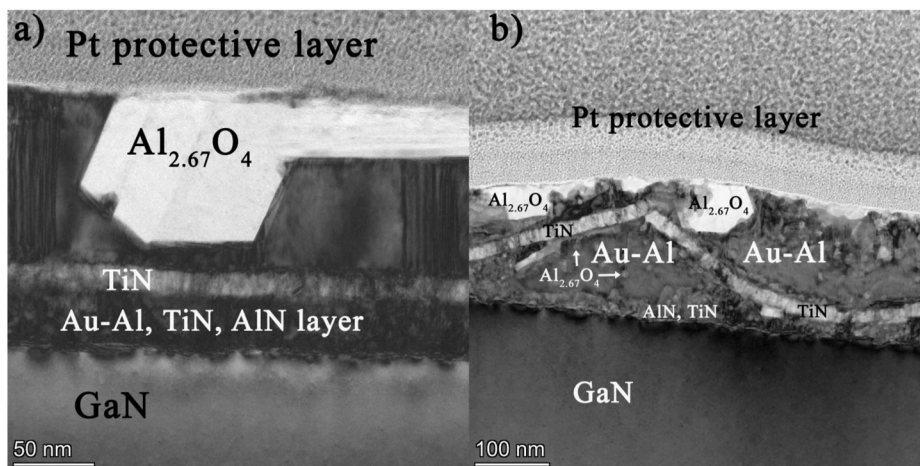
Fig. 4. BF TEM images of the heat-treated sample containing 15 nm "initial" TiN. In the BF TEM image a) the "initial" TiN is parallel to the GaN substrate, while the BF TEM image b) was taken from an area of the sample where the "initial" TiN layer rippled because in this area a larger amount of Au diffused through the "initial" TiN layer.
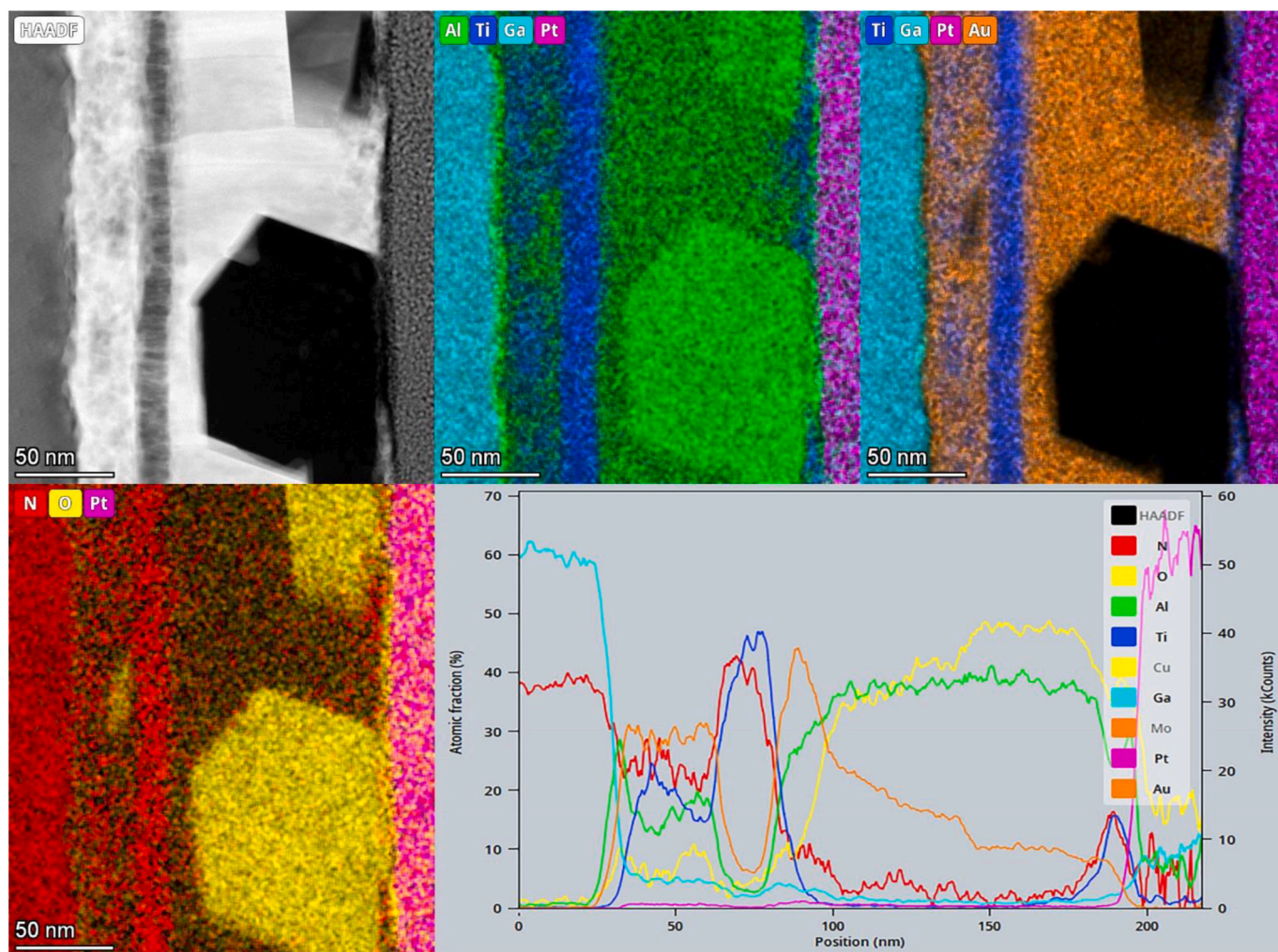

Fig. 5. HAADF image and EDS elemental maps obtained from the heat-treated sample containing 15 nm "initial" TiN of an area where the "initial" TiN remained parallel to the GaN after heat treatment.

The (scanning) transmission electron microscopy ((S)TEM) investigations were carried out in an aberration corrected THEMIS type transmission electron microscope operating at 200 keV. For the energy dispersive X-ray (EDX) mapping a Super-X detector was used. The cross-sectional TEM samples were prepared by a focused ion beam (FIB) technique. In the case of the samples with a TiN layer of 60 and 90 nm
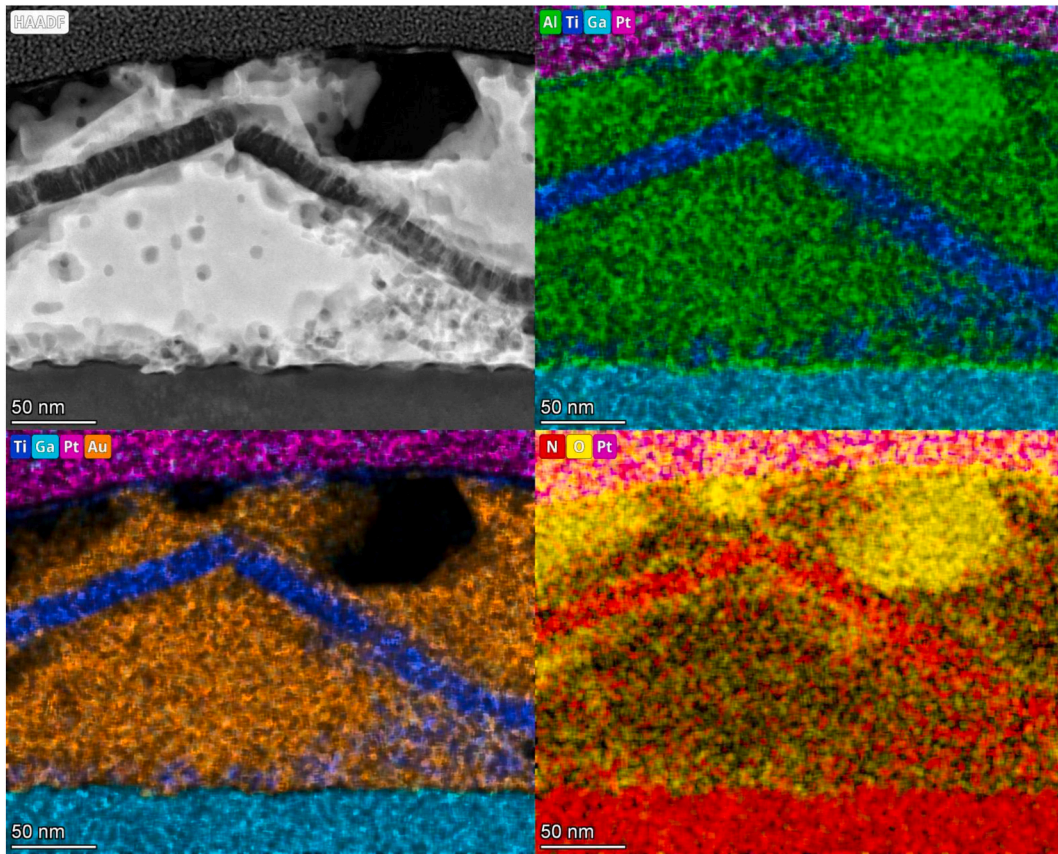
Fig. 6. HAADF image and EDS elemental maps obtained from the heat-treated sample containing 15 nm "initial" TiN of an area where the "initial" TiN rippled due to heat treatment.

Fig. 7. HAADF image and EDS elemental maps obtained from the heat-treated sample containing 15 nm "initial" TiN of an area, where the "initial" TiN rippled due to heat treatment and in some areas the "initial" TiN layer approaches the contact surface by a few nm.
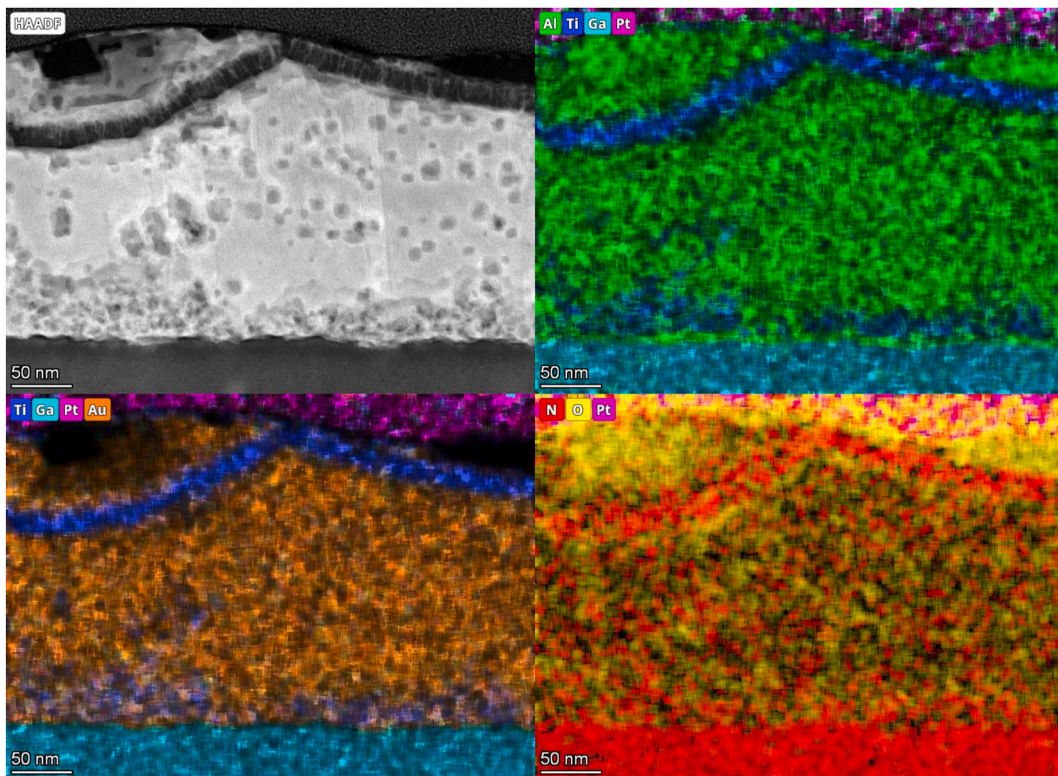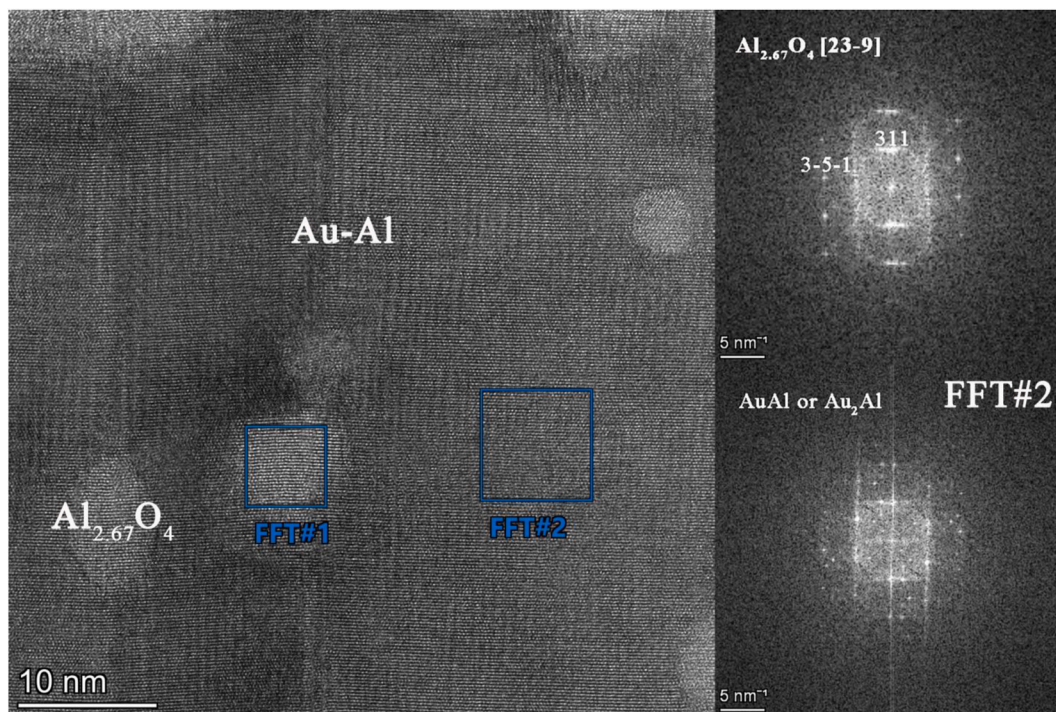
Fig. 8. HRTEM image of the Au–Al alloy and the epitaxial $Al_{2.67}O_4$ structure of the precipitates located in the area between the "initial" TiN layer and the GaN substrate in the heat-treated sample containing 15 nm "initial" TiN.
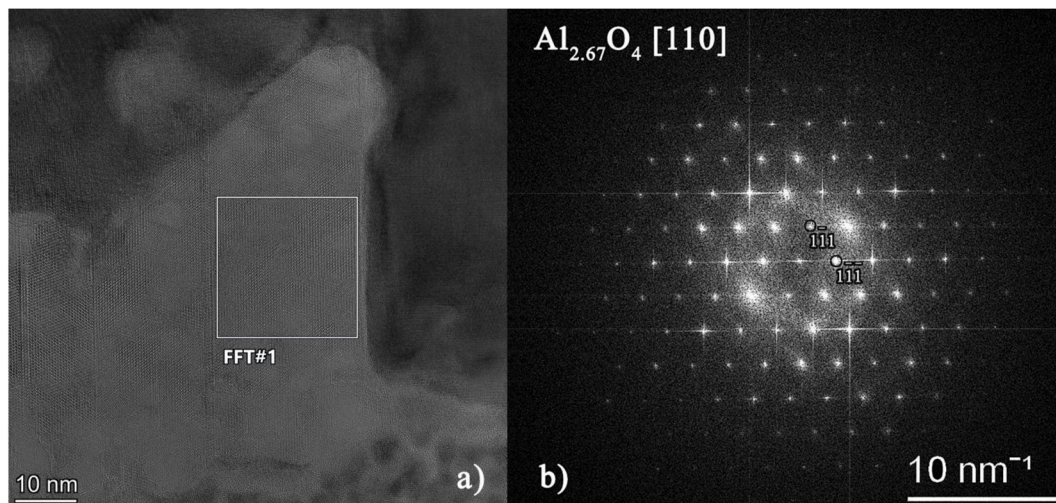

Fig. 9. HRTEM image a) and selected area FFT b) of an $Al_{2.67}O_4$ grain in the Au–Al and $Al_{2.67}O_4$ layer from the surface of the contact layer (from the heat-treated sample containing 15 nm "initial" TiN).

thickness, the upper gold layer was removed in aqua regia for 30 s before the preparation of the TEM sample as it was easier to produce a better quality TEM sample in such way. The gold layer above the TiN was examined only in the case of sample without heat treatment and in the case of heat treated sample with a 15 nm thick TiN layer.

3. Results

3.1. I–V curves

Initially, the I–V curves are asymmetric with low currents in the range below 20 mA at -2V bias and 100 mA at 1.5 V (see Fig. 1). The annealing at temperatures of 200–300 °C causes a drop in the current values. Increasing the temperature to 400–500 °C causes a surge in the positive polarization current, reaching 500 mA at 2 V, with the negative current rising to around 70 mA for -2 V. Heat treatment at 600 °C and at higher temperatures causes a more symmetric I–V curve relative to the OY axis and higher currents at low polarizations. At 750 °C the ohmic contact is formed with a fully symmetric profile and high currents at very low polarizations. A similar curve is obtained for the thicker TiN layers, however using the cTLM method, it was impossible to compare the exact values of contact resistivities due to the very low values. The layers heat-treated at 750 °C behaved as good ohmic contact and showed minimal differences in the I–V curves compared to each other (see Fig. 1).
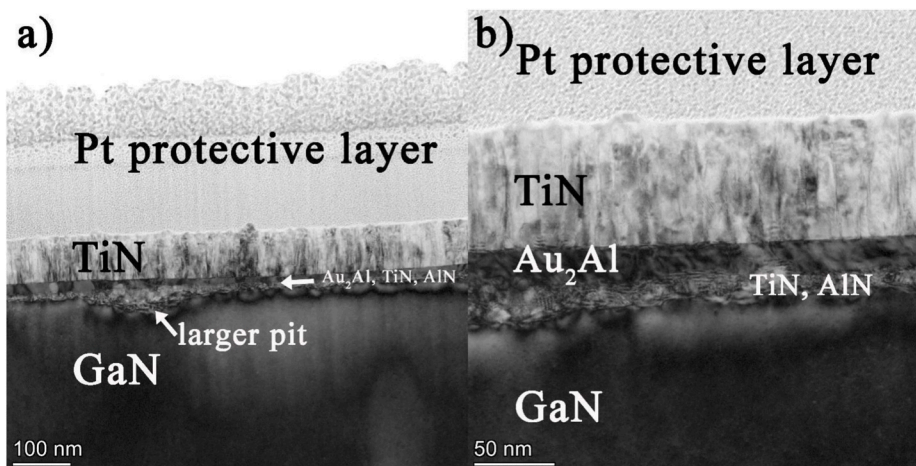
Fig. 10. BF TEM images of the heat-treated sample containing 60 nm "initial" TiN. Comparing the as-deposited sample to the smooth GaN substrate surface pits appear in the heat-treated sample on the GaN substrate (a). However, there are areas where the layer system has a relatively continuous thickness and arrangement (b).
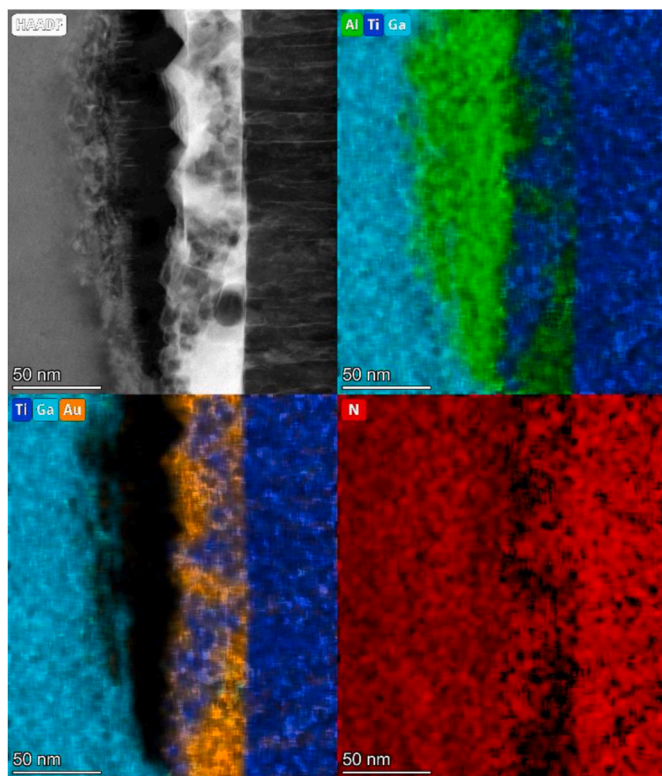

Fig. 11. HAADF image and Al, Ti, Ga, Au, N elemental maps of the heat-treated 60 nm thick "initial" TiN sample in the vicinity of a pit on the GaN surface. The pit on GaN surface is filled with AlN. TiN grains are located in the Au$_2$Al layer above the pit.

3.2. TEM and XRD investigations

3.2.1. As-deposited sample

For investigating the state of the GaN/metal interface after deposition and whether any intermixing took place at the other interfaces, we studied the as-deposited sample containing 15 nm TiN. In the sample a 15 nm thick Ti layer is located on the surface of the GaN substrate, as shown in Fig. 1. The Ti layer is followed by a 44 nm thick Al layer, then a 14 nm thick TiN layer is deposited on the Al layer. The thickness of the

Au layer on the TiN surface was 82 nm based on the TEM and the STEM-EDS measurements (Fig. 2). The TEM investigations has shown that the layers have a strong texture, in some areas the layers are epitaxial to each other. Moreover, according to the XRD patterns, only a single prominent reflection can be observed from the planes of each deposited layers, those that are parallel to the surface over large areas (Fig. 3).

3.2.2. The sample containing 15 nm thick TiN after heat treatment at 750 °C

Bright field (BF) TEM images of the sample with an initial TiN thickness of 15 nm are shown in Fig. 4. The surface of the GaN substrate is relatively smooth, but pits can be seen, with the size of few nanometers as shown in Fig. 4a. The BF TEM image of a larger structure, shown in Fig. 4b shows that the sample has a high degree of inhomogeneity. This inhomogeneity can be traced mostly in the shape of the TiN layer, which was initially parallel to the substrate surface. The TiN layer in the heat treated sample exhibits the same crystalline structure and thickness as the "initial" TiN proving the thermal stability of TiN itself, but it is no longer uniformly parallel to the substrate or continuous. In some areas, the "initial" TiN layer is parallel to the GaN substrate (see Figs. 4a and 5). In other areas, the "initial" TiN has rippled (Fig. 6), even to such an extent that some parts are approaching the contact surface by a few nm. (Fig. 7). This inhomogeneity is due to the fact that Au and Al diffused through the TiN layer as a result of the heat treatment, but not homogeneously, *i.e.* in some areas a larger amount of Au passed through the TiN layer, so the Au could push up the initial TiN layer in that area. Al and Au alloys were formed both under the initial TiN layer and above. Part of the Al collected the oxygen in the layer and on the upper side of the initial TiN (on the GaN substrate side) epitaxially aligned precipitates were formed in the Au–Al matrix with a spinel Al$_{2.67}$O$_4$ structure of a few nm (see Fig. 8). At the same time, more oxygen was available on the upper side of the initial TiN layer (on the surface side of the contact), here grains around 100 nm with a structure of Al$_{2.67}$O$_4$ can be observed, which can also reach the surface of the contact (see Figs. 4, 5 and 9). The Al$_{2.67}$O$_4$ grains can create significant bulges (5–10 nm) on the contact surface, which can explain the earlier findings, that the Au layer can make the surface morphology rough during the heat treatment [6]. On the surface of the GaN substrate, an AlN layer with a thickness of 1–2 nm is located relatively homogeneously. Above the AlN layer, TiN grains created by the heat treatment and Au–Al alloy grains can be also observed. The location and thickness of this mixed layer varies from area to area depending on how much Au has diffused to that area through the initial TiN layer (see Figs. 5–7).
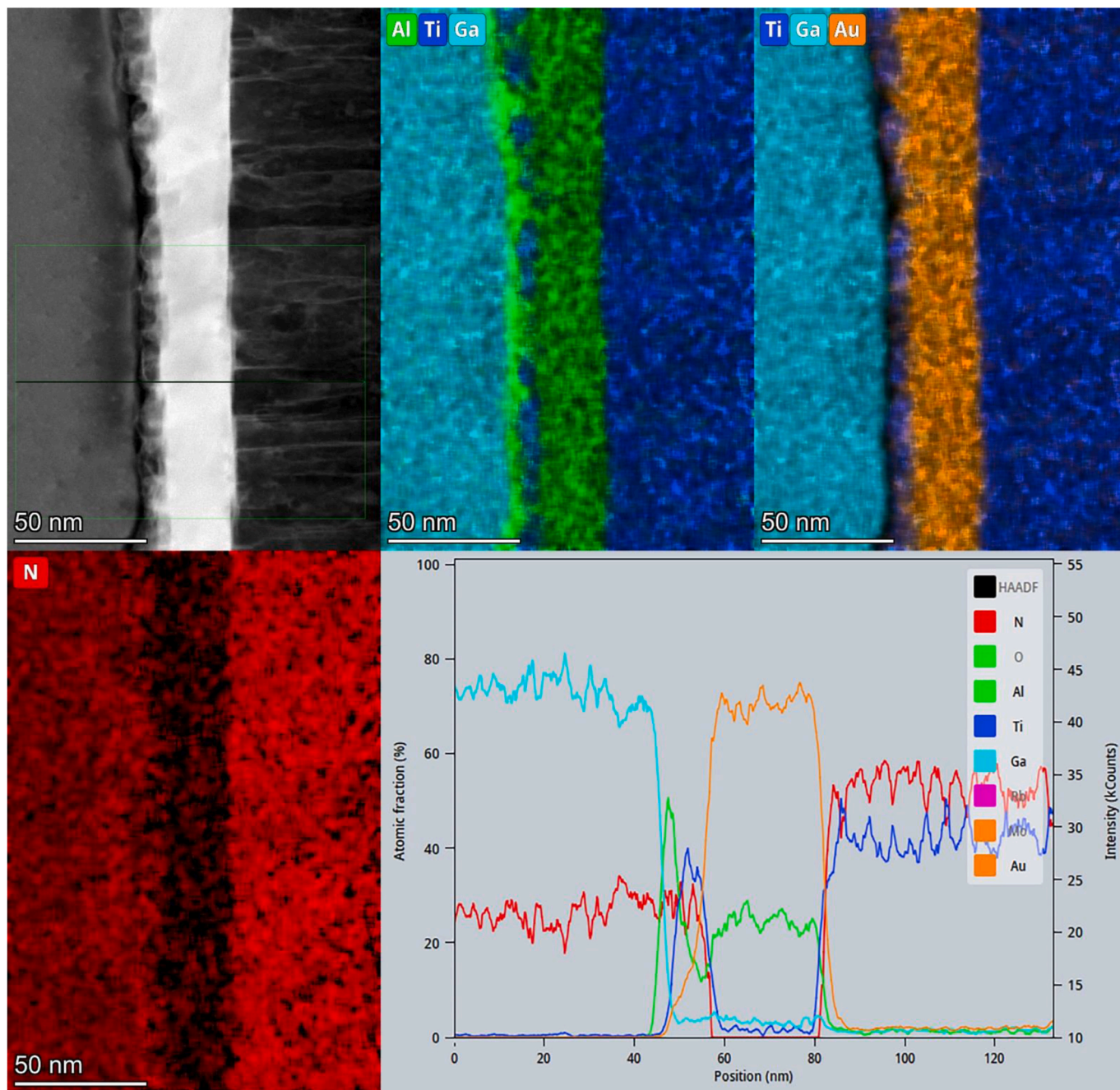
Fig. 12. HAADF image, Al, Ti, Ga, Au, N element maps, as well as the integral of the element distribution parallel to the surface of the heat-treated sample containing 60 nm "initial" TiN from an area where no pits were observed on the GaN surface is shown. A few nm AlN layer can be observed on the GaN surface, followed by a few nm TiN layer, which is not perfectly continuous. The Au_2Al layer is located on the TiN layer, followed by the "initial" TiN layer.

3.2.3. The sample containing 60 nm thick TiN after heat treatment at 750 °C

The surface of the GaN substrate is mostly smooth in the examined area (Fig. 10), however, in some areas pits with a depth of 10–30 nm can be observed on the surface of GaN (Figs. 10 and 11). On the GaN surface, a few nm thick Al and N-rich layer (according to the TEM structure measurements it can be AlN) followed by also a few nm thick Ti and N-rich layer (the structure can be TiN based on TEM investigations) can be observed by the EDS measurements on Fig. 12. Near the pits, slightly thicker AlN forms. The TiN layer is followed by an approx. 17 nm thick Au–Al alloy layer (Fig. 12), which is narrower above the pits observed on the GaN substrate. Above the pits in the AuAl alloy layer TiN grains can be seen in the EDS maps (Fig. 11) and in the HRTEM images (Fig. 13).

This layer is followed by an approx. 74 nm thick TiN layer (this is the "initial" TiN layer). The "initial" TiN layer is epitaxial to the substrate, however, in both HAADF and HRTEM images fainter lines in the TiN layer perpendicular to the substrate can be observed which separate areas with different orientations by a few degrees. This slight misorientation over large areas has shown up in the FFT and in diffraction patterns as a circular broadening of the reflections.

3.2.4. The sample containing 90 nm thick TiN after heat treatment at 750 °C

The order of the layers is the same, but uneven areas (pits) are more frequent on the surface of the GaN substrate than in the case of the sample with 60 nm thick "initial" TiN layer (see Figs. 10 and 14).
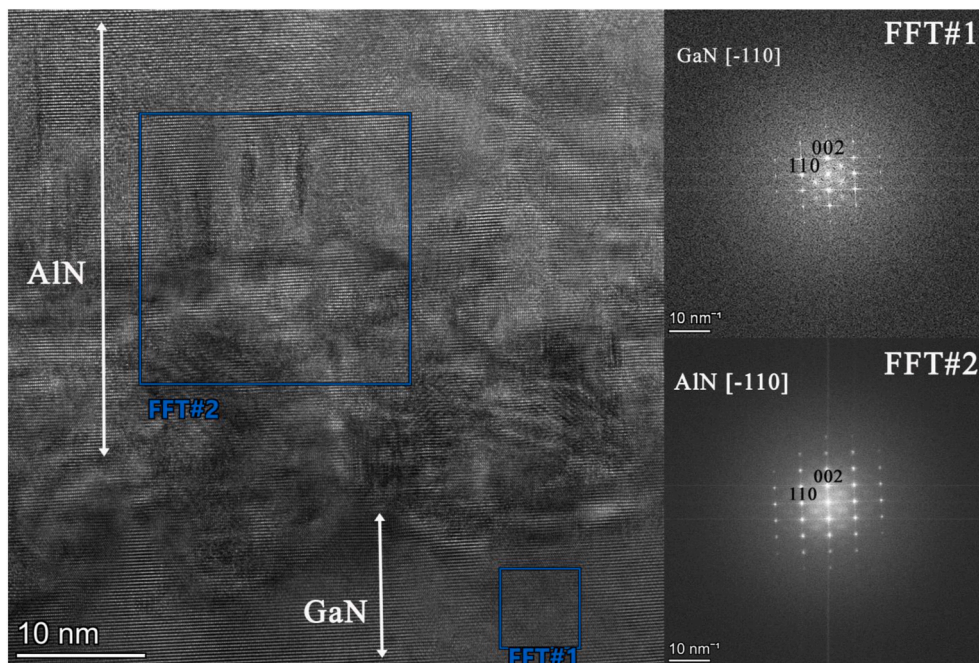
Fig. 13. HRTEM image of the heat-treated 60 nm thick "initial" TiN sample from the pit on the surface of a GaN. The pit in GaN surface is filled by epitaxially oriented AlN.
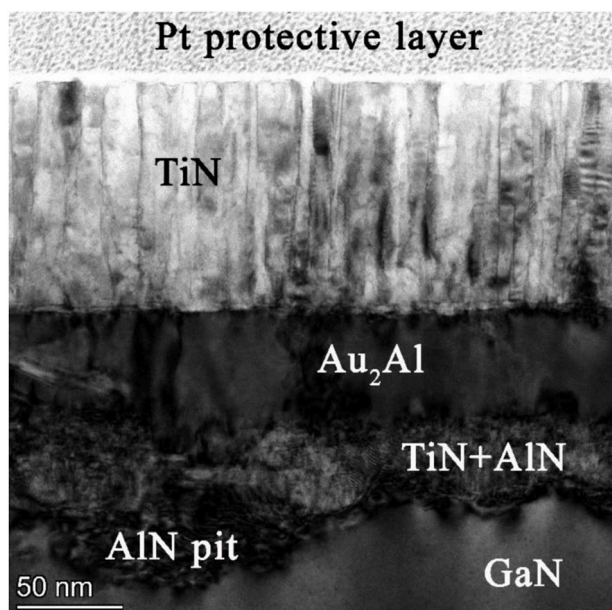

Fig. 14. BF TEM image of the heat-treated sample containing 90 nm "initial" TiN.

Interestingly, the alloy layer is much thicker than that observed for the sample with a 60 nm "initial" TiN layer and they might differ slightly in composition, as well (Fig. 15). It can be concluded that due to the thicker TiN layer (in the case of the sample with 60 and 90 nm thick "initial" TiN layer), it is more difficult for Al to reach the surface, but more Au can be bound in the alloying layer because more Al is present. The excess of etchings observed on the surface may be the result of Al having more time to form AlN, as the "initial" TiN layer requires more time for Au to diffuse through it and bond the Al. Based on the HRTEM observations, the layers forming the contact layers are located epitaxially on top of each other (Fig. 16), this observation coincides with the one observed in

XRD patterns, which explains the fact that there is only one XRD reflection measured for each layer. An exception is the Au–Al alloy phase, which can presumably contain several types of epitaxial orientation relationships with the neighboring layers. Fig. 17 shows HRTEM images obtained from Al–Au layer between TiN and GaN with corresponding FFTs from two different zone axis with ~30° tilt between them. The layer shows orthorhombic Au_2Al structure with *Pnma* s.g. with unit cell parameters of a = 6.715 Å, b = 3.219 Å, c = 8.815 Å. Au_2Al shows twinning (see. Fig. 17b) and the layer is thick, therefore Moiré pattern of the twins is observed.

4. Discussion

Based on the results of the measurements, the surface of GaN substrate was roughened during the heat-treatment at 750 °C, i.e. the surface of the substrate mixed with the contact layer. A part of the Ti and Al layer previously located on the substrate was transformed into TiN and a part into AlN. For enabling this transformation to take place, some of the N had to diffuse out from the GaN. A small amount of Ga may also have separated from the GaN substrate, which can presumably be located in the Au_2Al dominated layer. However, it is difficult to prove this, since the better scattering areas can also excite the GaN substrate during the STEM EDS examination and a small amount of Ga may have entered the sample during FIB thinning of the TEM samples therefore small amounts of Ga cannot be localized with high certainty. Precipitations with a large amount of Ga content could not be localized in the samples. The supposed diffusion processes are illustrated in Fig. 18.

As expected based on the literature presented in the introduction [17–19], TiN did not behave as a diffusion boundary layer, *i.e.* both Al and Au diffused through the TiN layer. On the lower, or substrate, side of the initial TiN layer, Au was able to form an Au_2Al alloy with the non-nitrided Al. However, on the other side of the initial TiN layer closer to the surface, Al could get a sufficient amount of oxygen, so it could form spinel $Al_{2.67}O_4$ crystals in the Au–Al alloy layer. Presumably, the presence of these $Al_{2.67}O_4$ crystals can cause the surface roughening observed by others [7] as a result of the heat treatment.

An epitaxial connection was observed for all of the layers formed during the heat treatment, however, in the initial TiN layer, the TiN
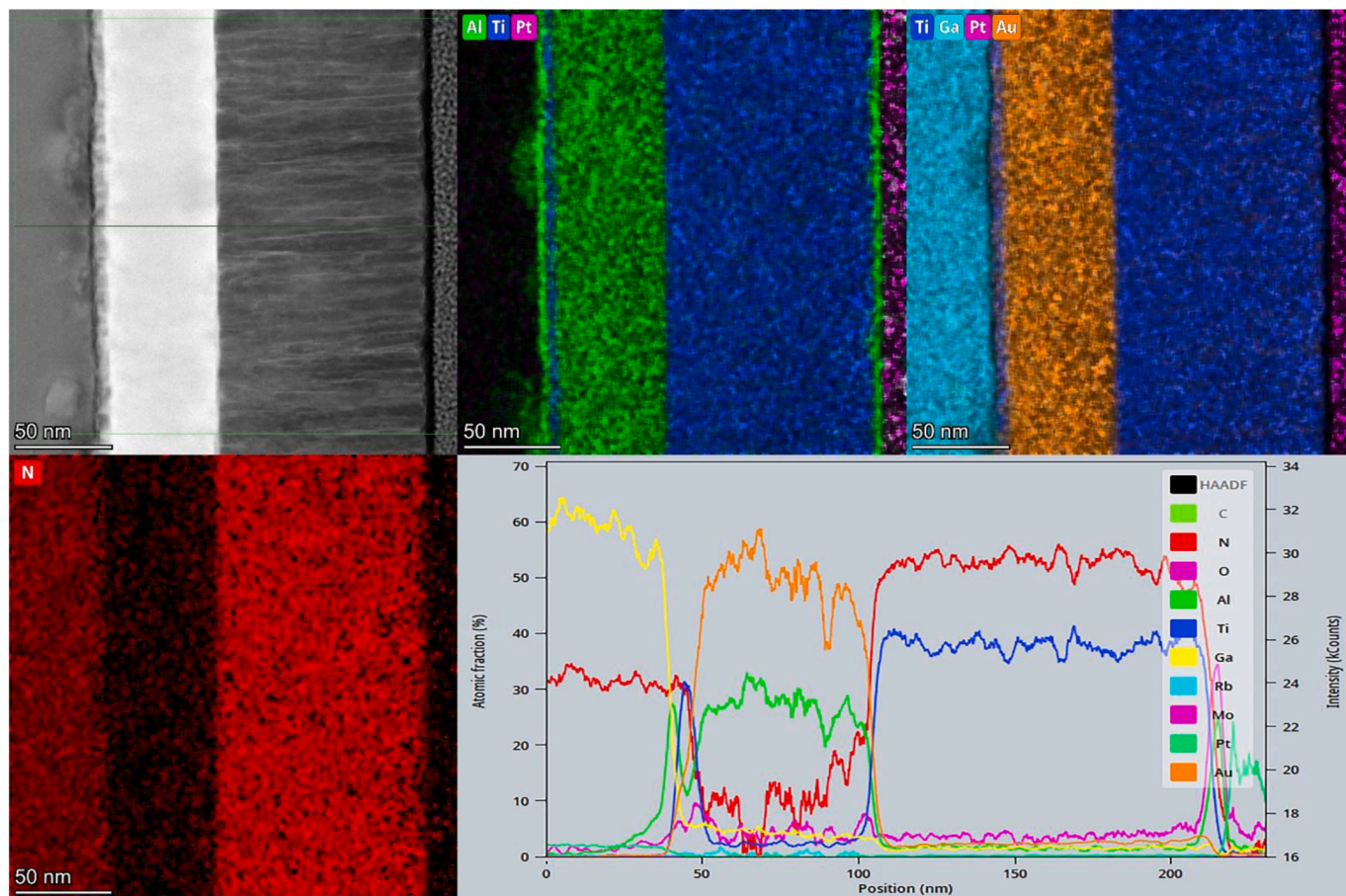
Fig. 15. HAADF image, Al, Ti, Ga, Au, N element maps, as well as the integral of the element distribution parallel to the surface of the heat-treated sample containing 90 nm thick "initial" TiN layer from an area where no pits were observed on the GaN surface is shown. A few nm AlN layer can be observed on the GaN surface, followed by a few nm TiN layer. The Au_2Al layer is located on the TiN layer, followed by the "initial" TiN layer.
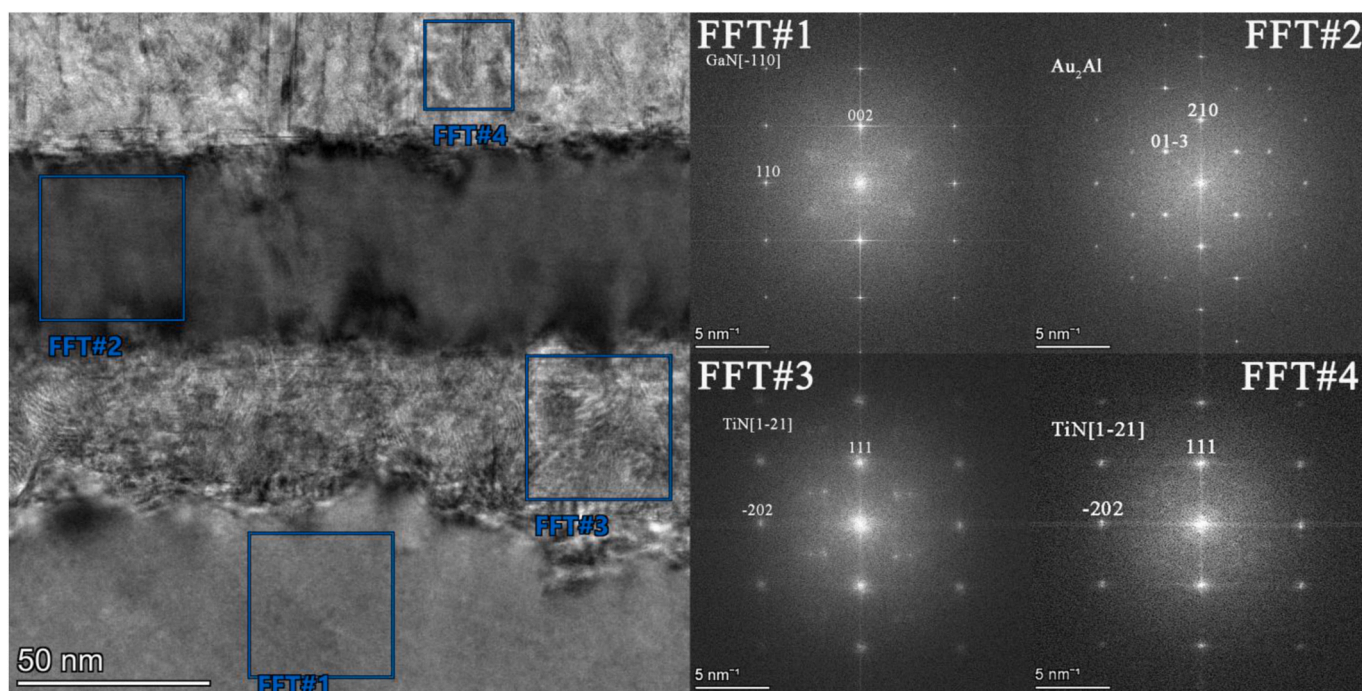

Fig. 16. BF TEM overview image of an area of the heat-treated sample containing 90 nm "initial" TiN with corresponding FFTs, where no prominently deep pit was observed on the GaN surface. Note: Au_2Al is close to [3−6−2] z.a., however slightly bit out of the zone with $d_{210}*$ vector (*i.e.* reflections with 1.42 Å and 1.97 Å come from another Laue-zone.).
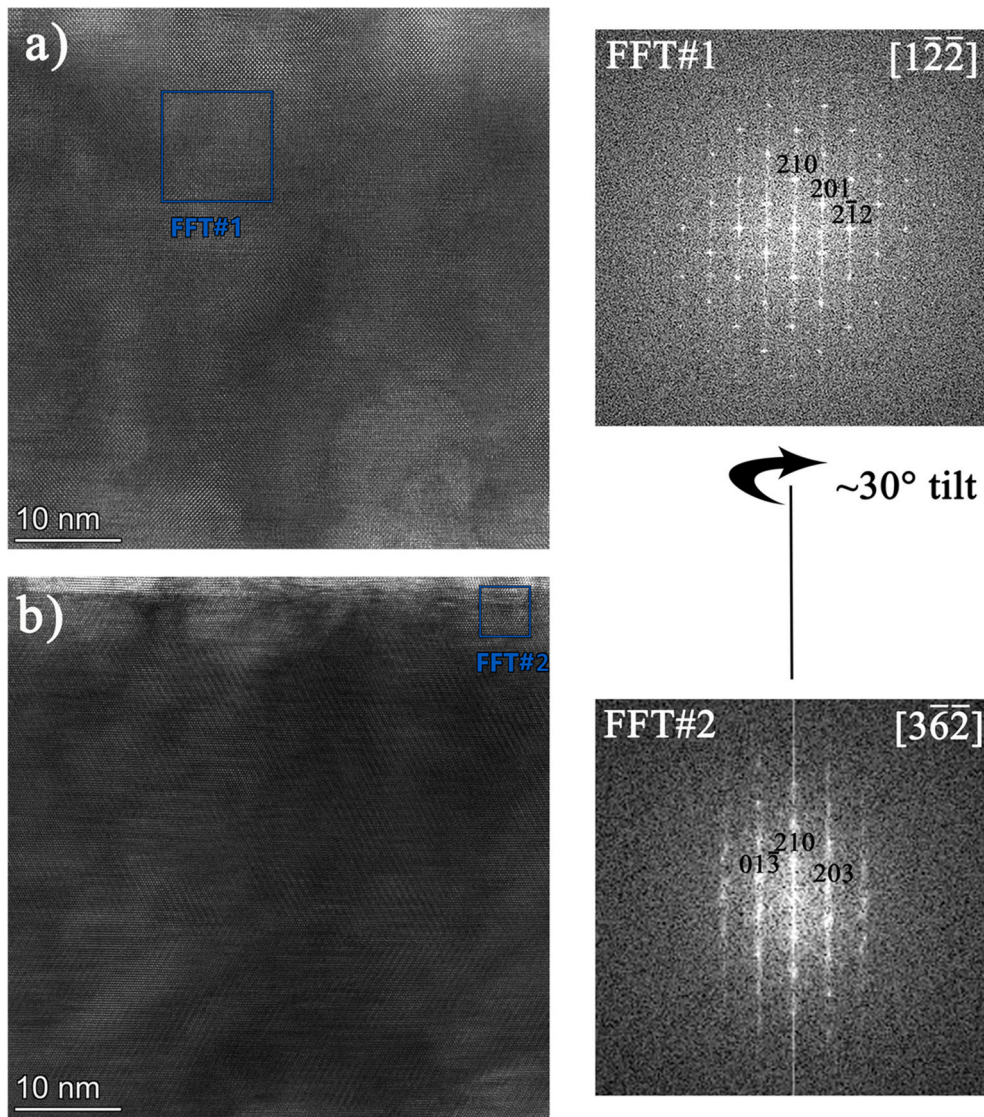
Fig. 17. HRTEM images and corresponding FFTs obtained from the Al–Au layer in sample containing 90 nm "initial" TiN from two different zone axis. The sample tilt between the two zone axis was approximately 30° around $\underline{d}_{210}*$. The layer is very thick, and show twinning and Moiré of different twin pairs clearly seen on the bottom image. FFT#2 was taken from where the layer is the thinnest avoiding overlapping of grains/twin pairs. This structure could be indexed as Au_2Al structure having orthorhombic *Pnma* structure with unit cell parameters of a = 6.715 Å, b = 3.219 Å, c = 8.815 Å. The angle between [1−2−2](a) and [3−6−2](b) zone axis is 29.9°.

(0001) planes closes an angle of approximately 1° to the surface of the substrate in the case of the samples with 60 or 90 nm thick initial TiN. The sign (±) of this angle can change from grain to grain in the heat-treated "initial" TiN layer, hence grain boundaries are formed in the "initial" TiN layer, which help the diffusion of Al and Au.

No significant difference in the formed layers could be observed between the samples with different initial TiN layer thicknesses. However, it was observed that in the case of the sample with thicker TiN, more and deeper pits were observed in the GaN substrate after the heat treatment, which can be explained by the fact that Al had more time to obtain nitrogen from the GaN substrate, due to the thicker TiN layer which hinders the mixing of Au with Al, effectively encapsulating Al on GaN. As a result, the pits on the GaN substrate surface were able to etch deeper in the case of the samples with thicker initial TiN layer. Another phenomenon was that in the case of the heat-treated sample with an initial TiN layer of 15 nm, the "initial" TiN rippled in some areas where a large amount of Au could diffuse through the TiN layer as a result of the heat treatment. Presumably, in some areas, the initial TiN layer may have larger defects in the sample with thinner TiN, along this defects

faster diffusion could take place. However, these did not affect the conductivity, as each contact layer had good ohmic properties, despite the fact that a few nm thick AlN was observed on the GaN surface for each heat-treated sample.

5. Conclusions

STEM investigations have shown that the traditional Ti/Al/TiN/Au contact layer deposited on the N-face of a single-crystal n-GaN substrate is transformed into an ohmic contact with the following layer structure: $AlN/TiN/Au_2Al/TiN/Au_2Al + Al_{2.67}O_4$ during heat treatment at 750 °C. During the heat treatment, the TiN layer had not been acted as a diffusion barrier layer therefore both Al and Au diffused through it. Spinel $Al_{2.67}O_4$ grains up to 100 nm in size could form in the upper initial Au layer resulting in surface roughening. A few nm thick AlN was formed on most of the surface of the GaN substrate, followed by a TiN layer. The explanation of the formation of these layers can be that N is separated from the GaN layer producing N vacancies in the GaN sub-strate. Non-nitrided Al forms an Au_2Al alloy with the Au diffused
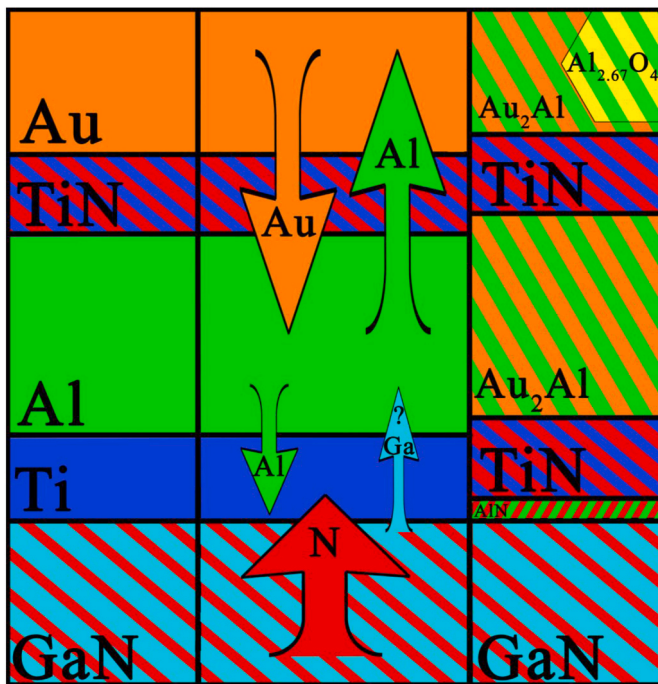
Fig. 18. The supposed diffusion processes during heat treatment.

through the "initial" TiN layer. Al–Ti alloys assumed in previous research were not observed. The interaction between the GaN and the contact layer was clearly supported by the fact that pits were formed on the surface of the GaN. The pits on the GaN surface were filled with AlN. By increasing the thickness of the "initial" TiN (15, 60, 90 nm), the number of pits and their size increased, which can be explained by the fact that Au needed more time to diffuse through the thicker TiN layer and bond the non-nitrided Al. Changing the thickness of the "initial" TiN had no effect on the conductivity of the contact layer formed after heat treatment as measured by cTLM method. All three contact layers with different initial TiN thicknesses behaved as good ohmic contact layers on the N-face of n-GaN substrate.

CRediT author statement

Z. Fogarassy: Investigation; Methodology; Supervision; Visualization; Writing - review & editing; Writing - original draft, A. Wójcicka: Investigation, I. Cora: Investigation; Methodology, Visualization, A.S. Racz: Writing –Review & Editing, Szymon Grzanka: Investigation, E. Dodony: Investigation; Visualization, Piotr Perlin: Resources, M.A. Borysiewicz - Funding acquisition, Supervision; Writing - review & editing.

Declaration of competing interest

The authors declare that they have no known competing financial interests or personal relationships that could have appeared to influence the work reported in this paper.

Data availability

Data will be made available on request.

Acknowledgements

References

[1] F. Roccaforte, G. Greco, P. Fiorenza, F. Iucolano, An overview of normally-off GaN-based high electron mobility transistors, Materials 12 (2019) 1599, https://doi.org/10.3390/ma12101599.

[2] R. Dimitrov, M. Murphy, J. Smart, W. Schaff, J.R. Shealy, L.F. Eastman, O. Ambacher, M. Stutzmann, Two-dimensional electron gases in Ga-face and N-face AlGaN/GaN heterostructures grown by plasma-induced molecular beam epitaxy and metalorganic chemical vapor deposition on sapphire, J. Appl. Phys. 87 (2000) 3375–3380, https://doi.org/10.1063/1.372353.

[3] M.E. Lin, Z. Ma, F.Y. Huang, Z.F. Fan, L.H. Allen, H. Morkoç, Low resistance ohmic contacts on wide band-gap GaN, Appl. Phys. Lett. 64 (1994) 1003–1005, https://doi.org/10.1063/1.111961.

[4] D.W. Jenkins, J.D. Dow, Electronic structures and doping of InN, $In_x Ga_{1-x}N$, and $In_xAl_{1-x}N$, Phys. Rev. B 39 (1989) 3317–3329, https://doi.org/10.1103/PhysRevB.39.3317.

[5] B.P. Luther, S.E. Mohney, T.N. Jackson, M. Asif Khan, Q. Chen, J.W. Yang, Investigation of the mechanism for Ohmic contact formation in Al and Ti/Al contacts to n-type GaN, Appl. Phys. Lett. 70 (1997) 57–59, https://doi.org/10.1063/1.119305.

[6] M. Nozaki, J. Ito, R. Asahara, S. Nakazawa, M. Ishida, T. Ueda, A. Yoshigoe, T. Hosoi, T. Shimura, H. Watanabe, Synchrotron radiation X-ray photoelectron spectroscopy of Ti/Al ohmic contacts to n-type GaN: key role of Al capping layers in interface scavenging reactions, Appl. Phys. Express 9 (2016) 105801, https://doi.org/10.7567/APEX.9.105801.

[7] A.N. Bright, P.J. Thomas, M. Weyland, D.M. Tricker, C.J. Humphreys, R. Davies, Correlation of contact resistance with microstructure for Au/Ni/Al/Ti/AlGaN/GaN ohmic contacts using transmission electron microscopy, J. Appl. Phys. 89 (2001) 3143–3150, https://doi.org/10.1063/1.1347003.

[8] F. Roccaforte, F. Iucolano, F. Giannazzo, A. Alberti, V. Raineri, Nanoscale carrier transport in Ti/Al/Ni/Au Ohmic contacts on AlGaN epilayers grown on Si(111), Appl. Phys. Lett. 89 (2006) 022103, https://doi.org/10.1063/1.2220486.

[9] E. Kamińska, A. Piotrowska, M. Guziewicz, S. Kasjaniuk, A. Barcz, E. Dynowska, M. D. Bremser, O.H. Nam, R.F. Davis, Ohmic contact to n-GaN with TiN diffusion barrier, MRS Online Proc. Libr. 449 (1996) 1055–1060, https://doi.org/10.1557/PROC-449-1055.

[10] V. Garbe, J. Weise, M. Motylenko, W. Münchgesang, A. Schmid, D. Rafaja, B. Abendroth, D.C. Meyer, Au-free ohmic Ti/Al/TiN contacts to UID n-GaN fabricated by sputter deposition, J. Appl. Phys. 121 (2017) 065703, https://doi.org/10.1063/1.4975485.

[11] B. Van Daele, G. Van Tendeloo, W. Ruythooren, J. Derluyn, M.R. Leys, M. Germain, The role of Al on Ohmic contact formation on n-type GaN and AlGaN/GaN, Appl. Phys. Lett. 87 (2005) 061905, https://doi.org/10.1063/1.2008361.

[12] S. Ruvimov, Z. Liliental-Weber, J. Washburn, K.J. Duxstad, E.E. Haller, Z.-F. Fan, S. N. Mohammad, W. Kim, A.E. Botchkarev, H. Morkoç, Microstructure of Ti/Al and Ti/Al/Ni/Au ohmic contacts for n-GaN, Appl. Phys. Lett. 69 (1996) 1556–1558, https://doi.org/10.1063/1.117060.

[13] L. Wang, F.M. Mohammed, I. Adesida, Differences in the reaction kinetics and contact formation mechanisms of annealed Ti/Al/Mo/Au Ohmic contacts on n-GaN and AlGaN/GaN epilayers, J. Appl. Phys. 101 (2007) 013702, https://doi.org/10.1063/1.2402791.

[14] L.L. Smith, R.F. Davis, R.-J. Liu, M.J. Kim, R.W. Carpenter, Microstructure, electrical properties, and thermal stability of Ti-based ohmic contacts to n-GaN, J. Mater. Res. 14 (1999) 1032–1038, https://doi.org/10.1557/JMR.1999.0137.

[15] J. Zhang, X. Kang, X. Wang, S. Huang, C. Chen, K. Wei, Y. Zheng, Q. Zhou, W. Chen, B. Zhang, X. Liu, Ultralow-contact-Resistance Au-free ohmic contacts with low annealing temperature on AlGaN/GaN heterostructures, IEEE Electron. Device Lett. 39 (2018) 847–850, https://doi.org/10.1109/LED.2018.2822659.

[16] Y.-F. Wu, W.-N. Jiang, B.P. Keller, S. Keller, D. Kapolnek, S.P. Denbaars, U. K. Mishra, B. Wilson, Low resistance ohmic contact to n-GaN with a separate layer method, Solid State Electron. 41 (1997) 165–168, https://doi.org/10.1016/S0038-1101(96)00151-7.

[17] M.Y. Kwak, D.H. Shin, T.W. Kang, K.N. Kim, Characteristics of TiN barrier layer against Cu diffusion, Thin Solid Films 339 (1999) 290–293, https://doi.org/10.1016/S0040-6090(98)01074-8.

[18] M. Mändl, H. Hoffmann, P. Kücher, Diffusion barrier properties of Ti/TiN investigated by transmission electron microscopy, J. Appl. Phys. 68 (1990) 2127–2132, https://doi.org/10.1063/1.346568.

[19] S. Kanamori, Investigation of reactively sputtered TiN films for diffusion barriers, Thin Solid Films 136 (1986) 195–214, https://doi.org/10.1016/0040-6090(86)90280-4.